The Journal of Physiological Sciences (2018) 68:103–111
https://doi.org/10.1007/s12576-017-0585-1

REVIEW

Lumped parameter model for hemodynamic simulation of congenital heart diseases

Shuji Shimizu[1] · Dai Une[1] · Toru Kawada[1] · Yohsuke Hayama[1] · Atsunori Kamiya[1] · Toshiaki Shishido[2] · Masaru Sugimachi[1]

Received: 19 July 2017 / Accepted: 5 December 2017 / Published online: 21 December 2017

Abstract
The recent development of computer technology has made it possible to simulate the hemodynamics of congenital heart diseases on a desktop computer. However, multi-scale modeling of the cardiovascular system based on computed tomographic and magnetic resonance images still requires long simulation times. The lumped parameter model is potentially beneficial for real-time bedside simulation of congenital heart diseases. In this review, we introduce the basics of the lumped parameter model (time-varying elastance chamber model combined with modified Windkessel vasculature model) and illustrate its usage in hemodynamic simulation of congenital heart diseases using examples such as hypoplastic left heart syndrome and Fontan circulation. We also discuss the advantages of the lumped parameter model and the problems for clinical use.

Keywords Lumped parameter model · Time-varying elastance · Windkessel model · Congenital heart diseases · Hemodynamic simulation

Introduction

Hemodynamic management of patients with congenital heart diseases remains a challenge for pediatric cardiologists and pediatric cardiac surgeons, and the number of specialists for pediatric hemodynamic management is limited. Recent development of computer technology has allowed simulations of hemodynamics of congenital heart diseases on desktop computers. The performance of a recent desktop computer has already reached a sufficient stage to perform some kind of real-time simulation.

There are two different approaches to simulating cardiovascular systems of congenital heart diseases. One approach is multi-scale computational fluid dynamics (CFD) modeling, which is often combined with lumped parameter models [1]. Modern imaging technologies such as three-dimensional computed tomography (CT) and magnetic resonance imaging (MRI) provide specific anatomical information of complex heart anomalies [2]. Hemodynamic simulation based on these anatomical data will be helpful for surgical decision making [3]. However, because large-scale computations are required to use these data, execution of the simulation process is too long to meet the requirement of real-time clinical applications [4]. Another approach is the simulation with a lumped parameter model, which can be performed even on a small bedside computer [5]. Although this type of hemodynamic simulation does not include specific anatomical information, the greatest advantage of this approach is that real-time simulation can be performed while acquiring clinical data from patients. This approach is likely to be more helpful for perioperative hemodynamic management.

In this review, we introduce computational modeling of congenital heart diseases using the lumped parameter model and discuss its usefulness and issues in clinical use.

✉ Shuji Shimizu
shujismz@ri.ncvc.go.jp

[1] Department of Cardiovascular Dynamics, National Cerebral and Cardiovascular Center, 5-7-1 Fujishiro-dai, Suita, Osaka 565-5685, Japan

[2] Department of Research Promotion, National Cerebral and Cardiovascular Center, 5-7-1 Fujishiro-dai, Suita, Osaka 565-8565, Japan

Lumped parameter model

The lumped parameter model of the cardiovascular system consists of two components; a time-varying elastance chamber component and a (modified) Windkessel vascular component. The time-varying chamber component describes instantaneous ventricular and atrial pressure–volume relations. The Windkessel vascular component describes hemodynamics in arterial and venous trees. The combination of these two components enables us to simulate the cardiovascular system; the left and right heart, and systemic and pulmonary circulations.

Time-varying elastance chamber component

In the lumped parameter model of cardiovascular system, each chamber (ventricle or atrium) is represented by a time-varying elastance model [6]. The basis of time-varying elastance chamber model has been reported by Suga et al. [7].

The chamber pressure at time (t) after onset of contraction is approximated as:

$$P(t) \cong E(t)[V(t) - V_0], \tag{1}$$

where t is the time after onset of contraction, $P(t)$ and $V(t)$ are instantaneous chamber pressure and volume, respectively, and V_0 is the volume axis intercept of the end-systolic pressure–volume relationship (ESPVR). $E(t)$ is an instantaneous elastance of the chamber, which is independent of the loading conditions. At end-systole (t_{es}), $E(t)$ reaches a maximal value (E_{es}), which is the slope of the ESPVR. Hence, ESPVR is described as:

$$P_{es}(t) = E_{es}[V_{es}(t) - V_0], \tag{2}$$

where P_{es} and V_{es} are end-systolic pressure and volume, respectively. In contrast with ESPVR, end-diastolic pressure–volume relationship (EDPVR) is often represented by an exponential curve:

$$P_{ed}(t) = A\{\exp[B(V_{ed}(t) - V_0)] - 1\}, \tag{3}$$

where P_{ed} and V_{ed} are end-diastolic pressure and volume, respectively. A and B are constants. The parameter B is called as a stiffness constant.

Instantaneous chamber pressure is described by the sum of P_{ed} and the developed pressure (difference between P_{es} and P_{ed}) scaled by normalized elastance curve [$e(t)$]:

$$P(t) = [P_{es}(V(t)) - P_{ed}(V(t))]e(t) + P_{ed}(V(t)). \tag{4}$$

Parameters E_{es}, V_0, A, and B are different among the four chambers (left and right ventricles and atria).

Elastance curve

In the real world, elastance curve ($E(t)$) looks like a skewed sine curve [8]. However, in computational simulation, the skewed sine curve is often replaced by a simple sine (or cosine) curve (Fig. 1a) [9, 10]:

$$\begin{aligned} e(t) &= 0.5[1 - \cos(\pi t/T_{es})]\ (0 \le t < 2T_{es}) \\ e(t) &= 0\ (2T_{es} \le t < T), \end{aligned} \tag{5}$$

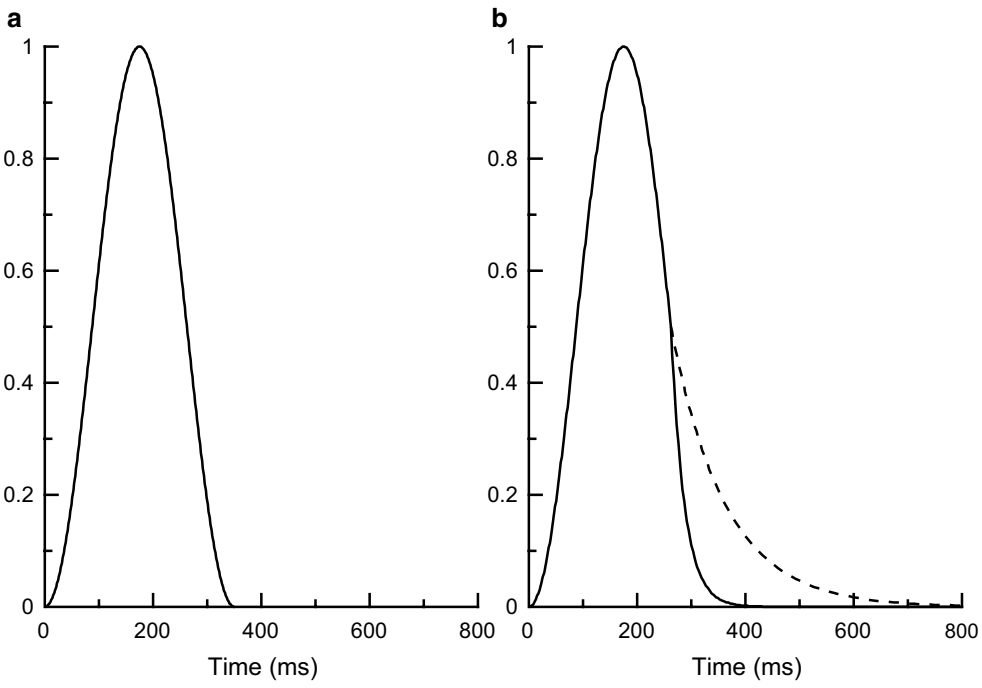

Fig. 1 Simulated normalized elastance curves (T_{es} = 175 ms). **a** A sine curve. **b** A sine curve combined with exponential curve. Time constant of relaxation (τ) is 25 ms for the *solid line* and 100 ms for the *dotted line*. An increase in τ prolongs the tail

where t is the time from the start of systole, T_{es} is the duration of systole, and T is the duration of cardiac cycle.

A sine curve combined with an exponential curve is also used as a normalized elastance curve (Fig. 1b) [11]:

$$\begin{aligned} e(t) &= 0.5[1+\sin(\pi t/T_{es}-\pi/2)]\,(0<t<3T_{es}/2)\\ e(t) &= 0.5\exp[(3T_{es}/2-t)/\tau]\,(3T_{es}/2\le t), \end{aligned} \tag{6}$$

where τ is the time constant of relaxation. An increase in τ prolongs the tail of the normalized elastance curve (Fig. 1b, dotted line). Because $e(t)$ is discontinuous from the end of one cardiac cycle to the beginning of the next, this may cause an error in the simulation result.

Windkessel vascular components

In the lumped parameter model of cardiovascular system, vasculatures are simulated as Windkessel vasculature models. There are three major vasculature models: two-, three-, and four-element Windkessel models [12]. The two-element Windkessel model consists of a resistor and a capacitor (Fig. 2a). The resistor represents vascular resistance and the capacitor represents vascular volume capacitance. In the three-element Windkessel model, another resistor corresponding to characteristic impedance (R_c) is serially added to the two-element Windkessel resistor and capacitor (Fig. 2b). In the four-element Windkessel model, an inductor is added to the three-element Windkessel model (Fig. 2c). There are several variations in the position of the inductor in the four-element Windkessel model [13].

When we consider the input impedance, the two-element Windkessel model is less accurate than the three- and four-element Windkessel models especially in the high-frequency range corresponding to the characteristic impedance. Since aortic and/or pulmonary characteristic impedances in patients with congenital anomaly dramatically change between before and after the surgical treatment, three- or four-element Windkessel model may be suitable for hemodynamic simulation of congenital heart diseases.

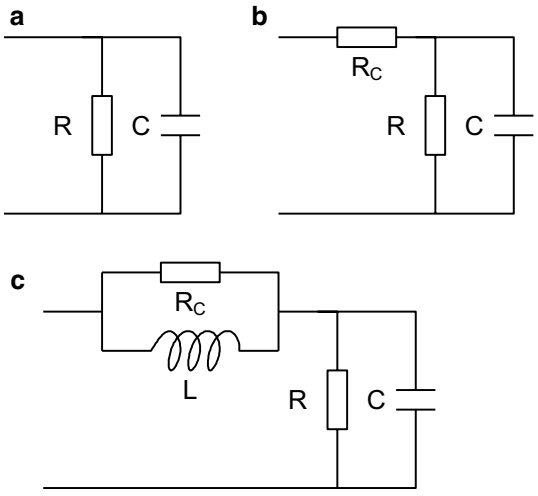

Fig. 2 Windkessel vasculature models. **a** Two-element model; **b** Three-element model; **c** Four-element model. R resistance, C capacitance, R_c characteristic impedance, L inductance

At each resistance (R), a linear relation between pressure drop (ΔP) and flow (Q) applies, according to the Ohm's law:

$$\Delta P = Q \cdot R. \tag{7}$$

At each capacitance (C), the relation between pressure (P) and volume (V), and the change in volume [$dV(t)/dt$] calculated by the difference between total inflow ($\sum Q_{inflow}$) and total outflow ($\sum Q_{outflow}$) are as follows:

$$P = \frac{V}{C}, \tag{8}$$

$$\frac{dV(t)}{dt} = \sum Q_{inflow}(t) - \sum Q_{outflow}(t). \tag{9}$$

At each inductance (L), the relation between pressure drop (ΔP) and change in flow [$dQ(t)/dt$] is as shown below:

$$\Delta P = L\frac{dQ(t)}{dt}. \tag{10}$$

Valves

Each valve (aortic, pulmonary, mitral, or tricuspid valve) is often represented as an ideal diode connected serially to a small resistor [14]. Several papers also used a diode connected with a non-linear resistance as a valve model [15], as described below:

$$\Delta P = k \cdot Q(t)^2. \tag{11}$$

Valve regurgitation is often simulated by introducing a second diode in the opposite direction with a small resistor [14].

Electrical analogs of cardiovascular systems

Using the framework of the time-varying elastance chamber model combined with the modified three-element Windkessel vasculature model, cardiovascular systems are described in terms of electrical analogs. Figure 3 shows the electrical analogs of the cardiovascular systems of a normal heart (Fig. 3a), Fontan circulation (total cavopulmonary connection, Fig. 3b), atrial septal defect (ASD, Fig. 3c), and ventricular septal defect (VSD, Fig. 3d).

In these electrical analogs, no non-linear components are used. However, non-linear components may sometimes be useful for hemodynamic simulation of congenital heart diseases as discussed below.

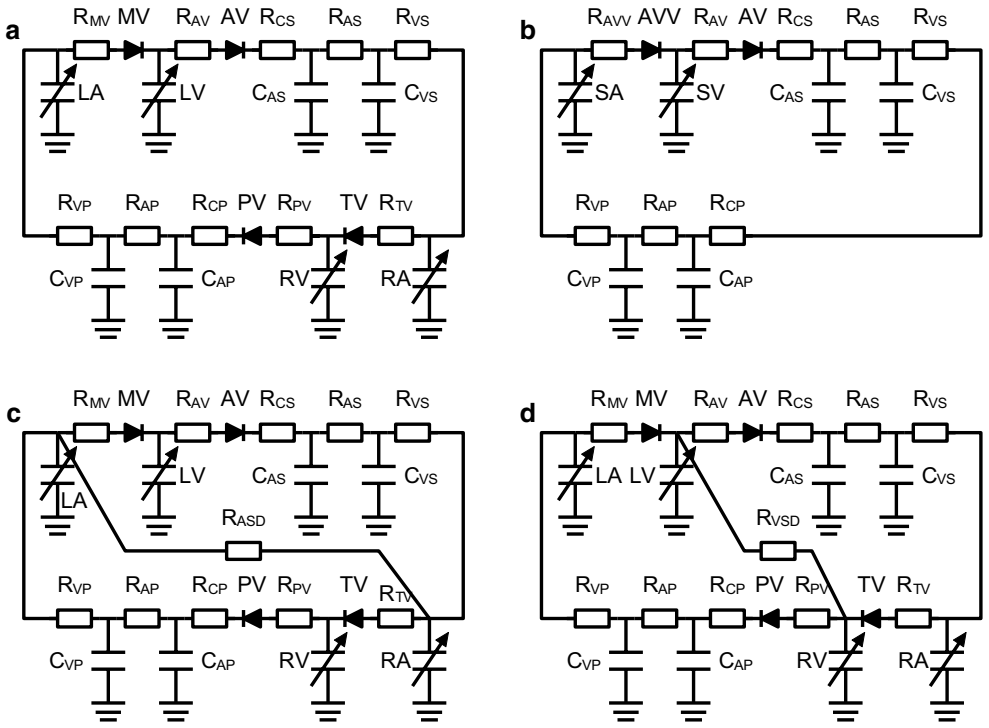

Fig. 3 Electrical analogs of cardiovascular systems of **a** normal heart, **b** Fontan circulation, **c** patient with atrial septal defect (ASD), and **d** patient with ventricular septal defect (VSD). *LA* left atrium, *LV* left ventricle, *RA* right atrium, *RV* right ventricle, *SA* single atrium, *SV* single ventricle, *MV* mitral valve, *TV* tricuspid valve, *AV* aortic valve, *PV* pulmonary valve, *AVV* atrioventricular valve. R_{CS}, R_{AS}, and R_{VS} denote systemic characteristic impedance, arterial resistance, and venous resistance, respectively. R_{CP}, R_{AP}, and R_{VP} denote pulmonary characteristic impedance, arterial resistance, and venous resistance, respectively. C_{AS} and C_{VS} denote pulmonary arterial and venous capacitances, respectively. C_{AP} and C_{VP} denote pulmonary arterial and venous capacitances, respectively. R_{ASD} and R_{VSD} denote the resistances across ASD and VSD, respectively

Non-linear components

In cardiovascular simulations of normal subjects and simple congenital heart diseases such as ASD and VSD, use of non-linear components may be unnecessary. However, hemodynamic simulation of some congenital heart diseases may require the use of non-linear components for modeling because shunt and stenosis behave non-linearly in clinical settings. To simulate these non-linear components, the Bernoulli's principle for the total hydraulic energy of an ideal fluid is important [16]. The general form of the Bernoulli's equation is;

$$P + \frac{1}{2}\rho v^2 + \rho gh = \text{constant}, \tag{12}$$

where P is pressure, v is blood velocity, ρ is blood density, g is acceleration of gravity, and h is height. The term ρgh can be neglected in many cases of hemodynamic simulation because the height difference across a shunt or stenosis is small. Addition of this equation in modeling may improve the accuracy of hemodynamic simulation of congenital heart diseases.

However, to simulate the fluid dynamics in non-linear components more accurately, multi-scale CFD modeling and solution of the Navier–Stokes equations are needed [17]. Because the numerical method (for example, the finite element method) is necessary to solve Navier–Stokes equations, the simulation may take time and is therefore unfavorable for bedside simulation. On the other hand, the Navier–Stokes equation may be required when we want to couple a structural model with a fluid dynamics model. As an example, in the case of the aortic arch reconstruction of the Norwood procedure, which accompanies structural changes in the aortic arch, we may not be able to predict postoperative hemodynamics from a preoperative lumped model. In such a case, a multi-scale CFD model with the Navier–Stokes equation would provide more accurate prediction of postoperative hemodynamics.

Solution of simultaneous equations

To simulate hemodynamics, solution of simultaneous equations (Eqs. 2, 3, 4, one of Eqs. 5 and 6, Eqs. 7, 8, 9, 10, Eqs. 11 and/or 12 where necessary) with given initial

parameters is necessary. The required initial parameters of chamber components are E_{es}, V_0, A and B for each chamber, T_{es}, and a delay between atrial and ventricular systole, which can be calculated from heart rate [18]. Initial parameters of vascular components are R_c, R, L, and C for each of the four vasculatures: systemic arterial, systemic venous, pulmonary arterial, and pulmonary venous vasculatures. In addition, the initial stressed blood volume, which is the sum of the initial volumes of all chambers and capacitors, is necessary. If non-linear components are used, these initial parameters are also needed to start the solution.

The simplest method to solve simultaneous equations is the Euler method, which is the first-order numerical procedure for solving differential equations with given initial values. When the first derivative of $y(t)$ ($\mathrm{d}y/\mathrm{d}t$) is described as a function of time (t) and $y(t)$,

$$\frac{\mathrm{d}y}{\mathrm{d}t} = f(t, y(t)),$$

$$y(t_0) = y_0,$$

where t_0 is the time of start and y_0 is the value of y at t_0. The time after n steps (t_n) is described using the step size (h):

$$t_n = t_0 + nh.$$

For the Euler method, one step from t_n to t_{n+1} is defined as:

$$\begin{aligned} y_{n+1} &= y_n + hf(t_n, y_n) \\ t_{n+1} &= t_n + h. \end{aligned} \tag{13}$$

Although this method is easy for programming, the accuracy is relatively low.

Local truncation error for the Euler method is proportional to h^2, while that for the fourth-order Runge–Kutta method is h^5. Therefore, fourth or higher order Runge–Kutta method may be favorable for the solution of simultaneous equations including non-linear components. Commercial software such as MATLAB/Simulink (The MathWorks, Inc. MA, USA) may be useful for solution using the high-order methods.

Hemodynamic simulation of congenital heart diseases

In this section, we introduce several examples of lumped parameter models used to simulate hemodynamics of congenital heart diseases such as hypoplastic left heart syndrome and Fontan circulation.

Modeling of hypoplastic left heart syndrome

Since hypoplastic left heart syndrome is one of the most serious congenital heart anomalies, many researchers are interested in hemodynamic simulation of hypoplastic left heart syndrome. Hemodynamic simulations of the Norwood procedure, a stage I palliation for hypoplastic left heart syndrome, are widely performed because the mortality of the procedure remains high (approximately 16%) even in 2017 [19] and hemodynamic assessments using computational models may improve its clinical outcome.

Migliavacca et al. [18] modeled the cardiovascular system after the original Norwood procedure with the modified Blalock–Taussig (BT) shunt, using a lumped parameter model combined with a non-linear BT shunt model. They examined the effects of shunt size, vascular resistances, and heart rate on the hemodynamics and oxygenation after the original Norwood procedure. Their simulation demonstrates that (1) larger shunts divert an increased proportion of cardiac output to the lungs, away from systemic perfusion, resulting in poorer O_2 delivery, (2) systemic vascular resistance exerts greater effect on hemodynamics than pulmonary vascular resistance, and (3) systemic arterial oxygenation is minimally influenced by heart rate changes.

In the Sano modification of the Norwood procedure, the BT shunt is replaced by a right ventricle-to-pulmonary artery shunt [20]. The Sano modification was also simulated using a lumped parameter model [21]. The electrical analog and simulated pressures of the Sano modification are shown in Fig. 4. In this simulation, the Sano modification, even using a non-valved conduit, is preferable to the original Norwood procedure from the viewpoint of ventricular energetics.

Researchers also have an interest in another type of stage I palliation; bilateral pulmonary artery (PA) bandings combined with ductal stenting (the so-called hybrid procedure). Young et al. [22] developed a lumped parameter model of the hybrid procedure and examined the effects of diameters of PA bandings and ductal stent on ventricular workload. In their model, larger PA banding diameter or a small stent diameter below 7 mm substantially increases ventricle workload and reduces systemic perfusion. Simulations were also used to compare the hybrid procedure and the Norwood procedures from the viewpoint of ventricular energetics [23]. Mechanical efficiency of the hybrid procedure is equivalent to that of the original Norwood procedure, but inferior to that of the Sano modification.

Modeling of Fontan circulation

Fontan operation is a surgical goal for patients with single ventricle physiology [24]. Although heart failure after the Fontan operation requires heart transplantation or ventricular

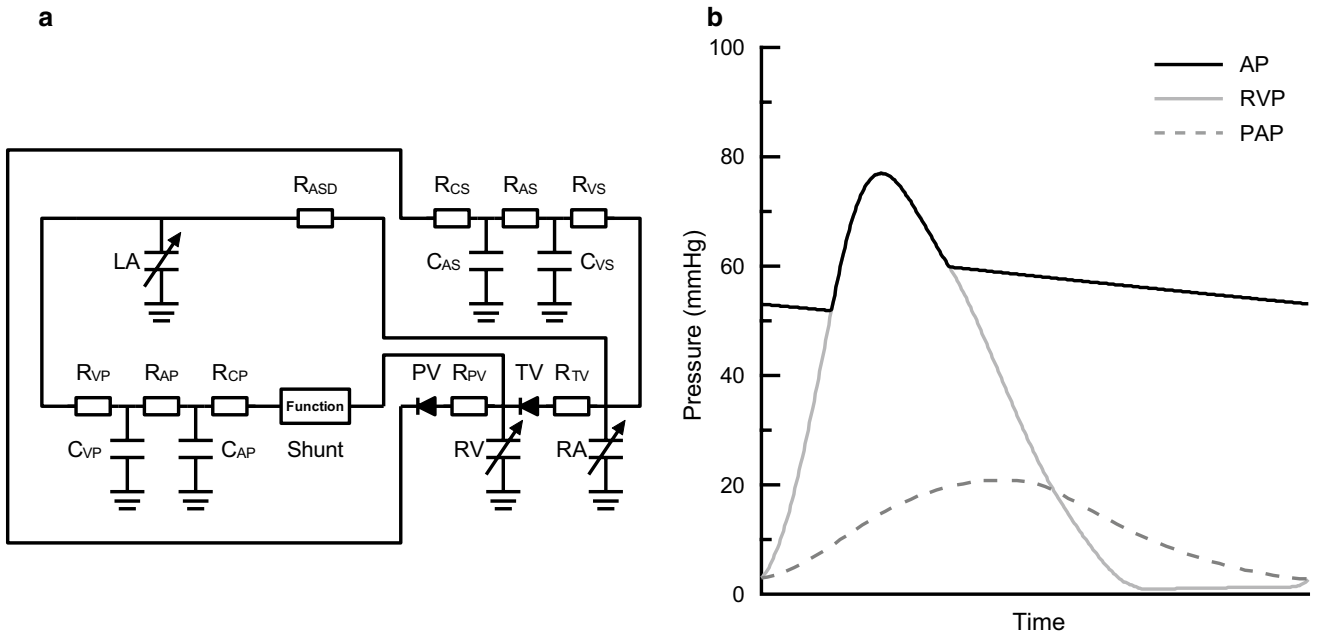

Fig. 4 **a** The electrical analog of the modified Norwood procedure with right ventricle (RV) to pulmonary artery (PA) shunt (Sano modification). The pressure gradient across the RV–PA shunt is described as a non-linear function. **b** Simulated aortic (*black solid line*), right ventricular (*gray solid line*) and pulmonary artery pressures (*gray dashed line*) of the Sano modification. *AP* aortic pressure, *RVP* right ventricular pressure, *PAP* pulmonary artery pressure

assist device (VAD) implantation, VAD implantation in Fontan patients remains a challenging issue in clinical settings [25]. Therefore, several researchers have investigated the effects of VAD on failing Fontan circulation [26–28]. Furthermore, reduced exercise capacity in Fontan patients is also a clinical interest, although the mechanism is not fully understood. Therefore, researchers also focus on exercise physiology in Fontan patients [29, 30].

Di Molfetta et al. [26] investigated the effects of cavopulmonary assistance (right-sided VAD) on the Fontan circulation using a lumped parameter model. They also examined the effects of combined use of continuous flow and pulsatile VAD on the Fontan circulation, and reported that left-sided continuous flow VAD concurrent with right-sided pulsatile VAD maximizes the hemodynamic benefits [27].

The effects of partial cavopulmonary assistance have also been examined using a lumped parameter model combined with a non-linear VAD model [28]. Partial cavopulmonary assistance from the inferior vena cava (IVC) to the pulmonary artery maintains cardiac index at lower IVC pressure but increases the superior vena cava pressure substantially, when compared with total cavopulmonary assistance from inferior and superior vena cavae to pulmonary artery.

Kung et al. [29] developed a closed loop lumped parameter model for simulation of exercise physiology in Fontan patients. Their model successfully reproduced the average exercise response of a cohort of typical Fontan patients. Based on the simulation results using a lumped parameter computational model, Koeken et al. [30] reported that exercise capacity in Fontan patients is limited due to an increase of central venous pressure and the incapability to further reduce systemic resistance, consequently restricting systemic flow.

Modeling of other congenital heart diseases

Effectiveness of the one and a half ventricle repair for hypoplastic right ventricle remains controversial in clinical settings. Several criteria of patient selection are based on anatomical factors such as *Z* score of the tricuspid valve and the right ventricular volume [31], but there are no accurate criteria based on physiological factors. A simulation study using a lumped parameter model reveals that the right ventricular stiffness constant (B) may predict the effectiveness of one and a half ventricular repair in improving postoperative hemodynamics [32].

The tetralogy of Fallot is one of the most common congenital heart anomalies, and is characterized by a ventricular septal defect, pulmonary stenosis, an overriding aorta and right ventricular hypertrophy. Kilner et al. [33] used a lumped parameter model to examine the factors influencing pulmonary regurgitation after repair of tetralogy of Fallot. They reported that pulmonary regurgitation was exacerbated by increased pulmonary artery compliance and by elevated pulmonary arteriolar resistance.

Advantages of hemodynamic simulation using the lumped parameter model

The major advantage of the lumped parameter model is that it requires shorter execution time even using a desktop computer. Although recent development of computer technology have enabled us to simulate hemodynamics of congenital heart diseases on desktop computers, simulation using a multi-scale CFD model is still time-consuming, and could take several days to complete [4]. In contrast to the multi-scale CFD model, the lumped parameter model may allow real-time simulation. This means that the lumped parameter model can be used to simulate patients' specific hemodynamics at the bedside under real-time data acquisition from the patients. Broomé et al. [34] reported the possibility of building a clinically relevant real-time computer simulation model of the normal adult cardiovascular system. Although several problems of applying a real-time computer simulation model to complex congenital anomalies remain to be solved, the usefulness of lumped parameter model in supporting clinical decision-making has been advocated [35].

Problems of hemodynamic simulation using the lumped parameter model

The lumped parameter model has the potential of simulating patient-specific hemodynamics at the bedside. However, there are several problems in clinical application. One of the most critical problems for bedside simulation is how to identify patient-specific (initial) parameters such as end-systolic elastance, resistances, inductances and compliances in clinical settings.

To identify systolic and diastolic chamber properties such as end-systolic elastance (E_{es}) and the stiffness constant (B), simultaneous monitoring of chamber pressure and volume is necessary. However, simultaneous measurement of chamber pressure and volume in clinical settings may be difficult even in adult patients without congenital heart anomaly. On the other hand, the recent development of imaging technologies such as knowledge-based reconstruction of three-dimensional echocardiographic images with MRI images may allow monitoring of chamber volume [36]. Combined with pressure data in the catheter laboratory, these volume data may be used in the estimation of chamber properties.

The three-element Windkessel parameters can be estimated in a time-domain and/or a frequency-domain manner from vascular pressure and flow waveforms [37, 38]. Furthermore, the method of beat-to-beat estimation of peripheral resistance (R) and arterial compliance (C) during transient conditions has been reported [39]. A technique to estimate the four-element Windkessel parameters for transient and steady beats has also been developed [40]. However, in contrast to the three-element Windkessel model, it may be difficult to identify the four-element Windkessel parameters, especially the inductances (L) [41]. Segers et al. reported that the four-element Windkessel model yielded the best quality of fit, but model parameters reached physically impossible values for L in about 12% of all cases [42]. Although an iterated unscented Kalman filter algorithm may improve estimation accuracy of four-element Windkessel parameters [43], further investigations are necessary to identify L with sufficient accuracy in every patients.

The direct estimation of venous capacitances and resistances is difficult in clinical settings as well as animal experiments. Therefore, several assumption of these values may be required at the start of the simulation and an algorithm to tune these values to physiologically proper values may be necessary.

In addition, estimation of all the parameters may take much time and may be invasive for patients with congenital heart diseases. Therefore, an algorithm that automatically estimates lumped parameters would be beneficial for clinical application of lumped parameter models. Schiavazzi et al. [44] attempted to develop a framework for automated tuning of lumped model parameters to match clinical data of patients after the Norwood procedure.

Instantaneous autonomic outflow at the estimation may affect lumped model parameters. Therefore, the results of hemodynamic simulation may depend on baseline autonomic nervous activities. In addition, global impairment of cardiac autonomic nervous activity is reported in patients after the operation of congenital heart diseases [45, 46]. How to incorporate the influence of autonomic nervous activities into the model remains an important matter. Furthermore, in children, body growth may also affect lumped model parameters. Therefore, re-identification of the parameters is necessary along with body growth. However, the model of cardiovascular system itself may be reusable.

Conclusions

The lumped parameter model is potentially beneficial for hemodynamic simulation of congenital heart diseases at the bedside because it allows real-time simulation. However, how to obtain patients' specific parameters remains a large obstacle for bedside simulation. Bedside simulation of congenital heart diseases can be realized if the problem of parameter identification can be solved.

Acknowledgements A part of this paper was presented at an award presentation at the 94th Annual Meeting of the Physiological Society of Japan, 2017.

Compliance with ethical standards

Funding This paper has been supported in part by a bounty of Hiroshi and Aya Irisawa Memorial Award for Excellent Papers on Research in Circulation in The Journal of Physiological Sciences.

Conflict of interest The authors declare that they have no conflicts of interest.

Ethical approval This paper was written focused on computational simulations. Therefore, there was no ethical approval.

References

1. Baker CE, Corsini C, Cosentino D, Dubini G, Pennati G, Migliavacca F, Hsia TY, Modeling of Congenital Hearts Alliance (MOCHA) Investigators (2013) Effects of pulmonary artery banding and retrograde aortic arch obstruction on the hybrid palliation of hypoplastic left heart syndrome. J Thorac Cardiovasc Surg 146:1341–1348
2. Riesenkampff E, Rietdorf U, Wolf I, Schnackenburg B, Ewert P, Huebler M, Alexi-Meskishvili V, Anderson RH, Engel N, Meinzer HP, Hetzer R, Berger F, Kuehne T (2009) The practical clinical value of three-dimensional models of complex congenitally malformed hearts. J Thorac Cardiovasc Surg 138:571–580
3. Corsini C, Baker C, Kung E, Schievano S, Arbia G, Baretta A, Biglino G, Migliavacca F, Dubini G, Pennati G, Marsden A, Vignon-Clementel I, Taylor A, Hsia TY, Dorfman A, Modeling of Congenital Hearts Alliance (MOCHA) Investigators (2014) An integrated approach to patient-specific predictive modeling for single ventricle heart palliation. Comput Methods Biomech Biomed Engin 17:1572–1589
4. Qian Y, Liu JL, Itatani K, Miyaji K, Umezu M (2010) Computational hemodynamic analysis in congenital heart disease: simulation of the Norwood procedure. Ann Biomed Eng 38:2302–2313
5. Jalali A, Jones GF, Licht DJ, Nataraj C (2015) Application of mathematical modeling for simulation and analysis of hypoplastic left heart syndrome (HLHS) in pre- and postsurgery conditions. Biomed Res Int 2015:987293
6. Hay I, Rich J, Ferber P, Burkhoff D, Maurer MS (2005) Role of impaired myocardial relaxation in the production of elevated left ventricular filling pressure. Am J Physiol Heart Circ Physiol 288:H1203–H1208
7. Suga H, Sagawa K, Shoukas AA (1973) Load independence of the instantaneous pressure–volume ratio of the canine left ventricle and effects of epinephrine and heart rate on the ratio. Circ Res 32:314–322
8. Shishido T, Hayashi K, Shigemi K, Sato T, Sugimachi M, Sunagawa K (2000) Single-beat estimation of end-systolic elastance using bilinearly approximated time-varying elastance curve. Circulation 102:1983–1989
9. Santamore WP, Burkhoff D (1991) Hemodynamic consequences of ventricular interaction as assessed by model analysis. Am J Physiol 260:H146–H157
10. Burkhoff D, Alexander J Jr, Schipke J (1988) Assessment of Windkessel as a model of aortic input impedance. Am J Physiol 255:H742–H753
11. Morley D, Litwak K, Ferber P, Spence P, Dowling R, Meyns B, Griffith B, Burkhoff D (2007) Hemodynamic effects of partial ventricular support in chronic heart failure: results of simulation validated with in vivo data. J Thorac Cardiovasc Surg 133:21–28
12. Westerhof N, Lankhaar JW, Westerhof BE (2009) The arterial Windkessel. Med Biol Eng Comput 47:131–141
13. Burattini R, Di Salvia PO (2007) Development of systemic arterial mechanical properties from infancy to adulthood interpreted by four-element Windkessel models. J Appl Physiol 103:66–79
14. Punnoose L, Burkhoff D, Rich S, Horn EM (2012) Right ventricular assist device in end-stage pulmonary arterial hypertension: insights from a computational model of the cardiovascular system. Prog Cardiovasc Dis 55:234–243.e2
15. Pennati G, Migliavacca F, Dubini G, Pietrabissa R, de Leval MR (1997) A mathematical model of circulation in the presence of the bidirectional cavopulmonary anastomosis in children with a univentricular heart. Med Eng Phys 19:223–234
16. Recordati G (1999) The contribution of the giraffe to hemodynamic knowledge: a unified physical principle for the circulation. Cardiologia 44:783–789
17. Mroczek T, Małota Z, Wójcik E, Nawrat Z, Skalski J (2011) Norwood with right ventricle-to-pulmonary artery conduit is more effective than Norwood with Blalock–Taussig shunt for hypoplastic left heart syndrome: mathematic modeling of hemodynamics. Eur J Cardiothorac Surg 40:1412–1417
18. Migliavacca F, Pennati G, Dubini G, Fumero R, Pietrabissa R, Urcelay G, Bove EL, Hsia TY, de Leval MR (2001) Modeling of the Norwood circulation: effects of shunt size, vascular resistances, and heart rate. Am J Physiol Heart Circ Physiol 280:H2076–H2086
19. Jacobs JP, Mayer JE Jr, Mavroudis C, O'Brien SM, Austin EH 3rd, Pasquali SK, Hill KD, Overman DM, St Louis JD, Karamlou T, Pizarro C, Hirsch-Romano JC, McDonald D, Han JM, Becker S, Tchervenkov CI, Lacour-Gayet F, Backer CL, Fraser CD, Tweddell JS, Elliott MJ, Walters H 3rd, Jonas RA, Prager RL, Shahian DM, Jacobs ML (2017) The Society of Thoracic Surgeons congenital heart surgery database: 2017 update on outcomes and quality. Ann Thorac Surg 103:699–709
20. Sano S, Ishino K, Kawada M, Arai S, Kasahara S, Asai T, Masuda Z, Takeuchi M, Ohtsuki S (2003) Right ventricle–pulmonary artery shunt in first-stage palliation of hypoplastic left heart syndrome. J Thorac Cardiovasc Surg 126:504–509
21. Shimizu S, Une D, Shishido T, Kamiya A, Kawada T, Sano S, Sugimachi M (2011) Norwood procedure with non-valved right ventricle to pulmonary artery shunt improves ventricular energetics despite the presence of diastolic regurgitation: a theoretical analysis. J Physiol Sci 61:457–465
22. Young A, Gourlay T, McKee S, Danton MH (2013) Computational modelling to optimize the hybrid configuration for hypoplastic left heart syndrome. Eur J Cardiothorac Surg 44:664–672
23. Shimizu S, Kawada T, Une D, Shishido T, Kamiya A, Sano S, Sugimachi M (2016) Hybrid stage I palliation for hypoplastic left heart syndrome has no advantage on ventricular energetics: a theoretical analysis. Heart Vessels 31:105–113
24. Walker SG, Stuth EA (2004) Single-ventricle physiology: perioperative implications. Semin Pediatr Surg 13:188–202
25. Jaquiss RD, Aziz H (2016) Is four stage management the future of univentricular hearts? Destination therapy in the young. Semin Thorac Cardiovasc Surg Pediatr Card Surg Annu 19:50–54
26. Di Molfetta A, Amodeo A, Fresiello L, Filippelli S, Pilati M, Iacobelli R, Adorisio R, Colella D, Ferrari G (2016) The use of a numerical model to simulate the cavo-pulmonary assistance in Fontan circulation: a preliminary verification. J Artif Organs 19:105–113
27. Di Molfetta A, Ferrari G, Iacobelli R, Filippelli S, Amodeo A (2017) Concurrent use of continuous and pulsatile flow ventricular

assist device on a Fontan patient: a simulation study. Artif Organs 41:32–39
28. Shimizu S, Kawada T, Une D, Fukumitsu M, Turner MJ, Kamiya A, Shishido T, Sugimachi M (2016) Partial cavopulmonary assist from the inferior vena cava to the pulmonary artery improves hemodynamics in failing Fontan circulation: a theoretical analysis. J Physiol Sci 66:249–255
29. Kung E, Pennati G, Migliavacca F, Hsia TY, Figliola R, Marsden A, Giardini A, MOCHA Investigators (2014) A simulation protocol for exercise physiology in Fontan patients using a closed loop lumped-parameter model. J Biomech Eng 136:0810071–08100714
30. Koeken Y, Arts T, Delhaas T (2012) Simulation of the Fontan circulation during rest and exercise. Conf Proc IEEE Eng Med Biol Soc 2012:6673–6676
31. Chowdhury UK, Airan B, Talwar S, Kothari SS, Saxena A, Singh R, Subramaniam GK, Juneja R, Pradeep KK, Sathia S, Venugopal P (2005) One and one-half ventricle repair: results and concerns. Ann Thorac Surg 80:2293–2300
32. Shimizu S, Shishido T, Une D, Kamiya A, Kawada T, Sano S, Sugimachi M (2010) Right ventricular stiffness constant as a predictor of postoperative hemodynamics in patients with hypoplastic right ventricle: a theoretical analysis. J Physiol Sci 60:205–212
33. Kilner PJ, Balossino R, Dubini G, Babu-Narayan SV, Taylor AM, Pennati G, Migliavacca F (2009) Pulmonary regurgitation: the effects of varying pulmonary artery compliance, and of increased resistance proximal or distal to the compliance. Int J Cardiol 133:157–166
34. Broomé M, Maksuti E, Bjällmark A, Frenckner B, Janerot-Sjöberg B (2013) Closed-loop real-time simulation model of hemodynamics and oxygen transport in the cardiovascular system. Biomed Eng Online 12:69
35. Di Molfetta A, Pilati M, Gagliardi MG, Fresiello L, Amodeo A, Cristofaletti A, Pongiglione G, Ferrari G (2015) Tailoring the hybrid palliation for hypoplastic left heart syndrome: a simulation study using a lumped parameter model. Med Eng Phys 37:898–904
36. Laser KT, Horst JP, Barth P, Kelter-Klöpping A, Haas NA, Burchert W, Kececioglu D, Körperich H (2014) Knowledge-based reconstruction of right ventricular volumes using real-time three-dimensional echocardiographic as well as cardiac magnetic resonance images: comparison with a cardiac magnetic resonance standard. J Am Soc Echocardiogr 27:1087–1097
37. Pochet T, Gerard P, Marnette JM, D'Orio V, Marcelle R, Fatemi M, Fossion A, Juchmes J (1992) Identification of three-element Windkessel model: comparison of time and frequency domain techniques. Arch Int Physiol Biochim Biophys 100:295–301
38. Shim Y, Pasipoularides A, Straley CA, Hampton TG, Soto PF, Owen CH, Davis JW, Glower DD (1994) Arterial Windkessel parameter estimation: a new time-domain method. Ann Biomed Eng 22:66–77
39. Toorop GP, Westerhof N, Elzinga G (1987) Beat-to-beat estimation of peripheral resistance and arterial compliance during pressure transients. Am J Physiol 252:H1275–H1283
40. Essler S, Schroeder MJ, Phaniraj V, Koenig SC, Latham RD, Ewert D (1999) Fast estimation of arterial vascular parameters for transient and steady beats with application to hemodynamic state under variant gravitational conditions. Ann Biomed Eng 27:486–497
41. Kind T, Faes TJ, Lankhaar JW, Vonk-Noordegraaf A, Verhaegen M (2010) Estimation of three- and four-element Windkessel parameters using subspace model identification. IEEE Trans Biomed Eng 57:1531–1538
42. Segers P, Rietzschel ER, De Buyzere ML, Stergiopulos N, Westerhof N, Van Bortel LM, Gillebert T, Verdonck PR (2008) Three- and four-element Windkessel models: assessment of their fitting performance in a large cohort of healthy middle-aged individuals. Proc Inst Mech Eng H 222:417–428
43. Huang H, Yang M, Zang W, Wu S, Pang Y (2011) In vitro identification of four-element Windkessel models based on iterated unscented Kalman filter. IEEE Trans Biomed Eng 58:2672–2680
44. Schiavazzi DE, Baretta A, Pennati G, Hsia TY, Marsden AL (2017) Patient-specific parameter estimation in single-ventricle lumped circulation models under uncertainty. Int J Numer Method Biomed Eng. https://doi.org/10.1002/cnm.2799
45. Davos CH, Davlouros PA, Wensel R, Francis D, Davies LC, Kilner PJ, Coats AJ, Piepoli M, Gatzoulis MA (2002) Global impairment of cardiac autonomic nervous activity late after repair of tetralogy of Fallot. Circulation 106:I69–I75
46. Davos CH, Francis DP, Leenarts MF, Yap SC, Li W, Davlouros PA, Wensel R, Coats AJ, Piepoli M, Sreeram N, Gatzoulis MA (2003) Global impairment of cardiac autonomic nervous activity late after the Fontan operation. Circulation 108:II180–II185